
Since January 2020 Elsevier has created a COVID-19 resource centre with free information in English and Mandarin on the novel coronavirus COVID-19. The COVID-19 resource centre is hosted on Elsevier Connect, the company's public news and information website.

Journal of Hazardous Materials 452 (2023) 131195

Contents lists available at ScienceDirect

Journal of Hazardous Materials

journal homepage: www.elsevier.com/locate/jhazmat

# A SERS-signalled, CRISPR/Cas-powered bioassay for amplification-free and anti-interference detection of SARS-CoV-2 in foods and environmental samples using a single tube-in-tube vessel

Long Ma [a,*], Wenlu Zhang [a], Lijuan Yin [a], Yaru Li [a], Jianwen Zhuang [a], Liang Shen [b,*], Shuli Man [a,*]

[a] State Key Laboratory of Food Nutrition and Safety, Key Laboratory of Industrial Microbiology, Ministry of Education, Tianjin Key Laboratory of Industry Microbiology, National and Local United Engineering Lab of Metabolic Control Fermentation Technology, China International Science and Technology Cooperation Base of Food Nutrition, Safety and Medicinal Chemistry, College of Biotechnology, Tianjin University of Science & Technology, Tianjin 300457, China
[b] Xiangyang Central Hospital, Affiliated Hospital of Hubei University of Arts and Science, Xiangyang 441000, China

## HIGHLIGHTS

- For the first time, a one-vessel, CRISPR-Cas12a powered SERS bioassay is developed for SARS-CoV-2 detection.
- This bioassay works in an amplification-free and anti-interference manner within 45 min
- The bioassay features a high detection sensitivity of 200 copies/mL, and the calculated LoD is down to 1.9 copies/mL.
- The established bioassay can be used for detecting pseudotyped SARS-CoV-2 in food and environmental samples.

## GRAPHICAL ABSTRACT

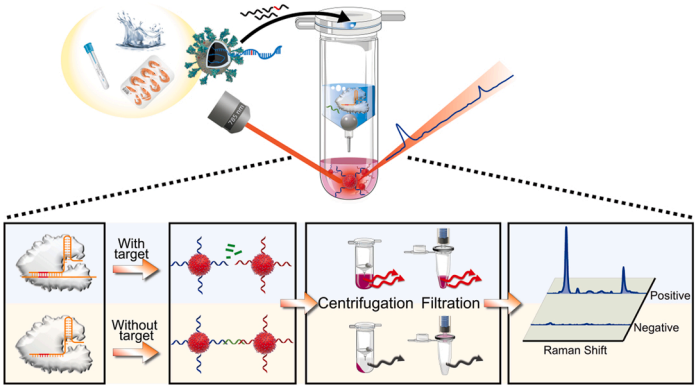


## ARTICLE INFO

Editor: Dr. Danmeng Shuai

*Keywords:*
CRISPR-Dx
Surface-enhanced Raman scattering
SARS-CoV-2
One-vessel detection
Amplification-free
Clinical and contaminated food samples

## ABSTRACT

The pandemic of COVID-19 creates an imperative need for sensitive and portable detection of SARS-CoV-2. We devised a SERS-read, CRISPR/Cas-powered nanobioassay, termed as OVER-SARS-CoV-2 (One-Vessel Enhanced RNA test on SARS-CoV-2), which enabled supersensitive, ultrafast, accurate and portable detection of SARS-CoV-2 in a single vessel in an amplification-free and anti-interference manner. The SERS nanoprobes were constructed by conjugating gold nanoparticles with Raman reporting molecular and single-stranded DNA (ssDNA) probes, whose aggregation-to-dispersion changes can be finely tuned by target-activated Cas12a though *trans*-cleavage of linker ssDNA. As such, the nucleic acid signals could be dexterously converted and amplified to SERS signals. By customizing an ingenious vessel, the steps of RNA reverse transcription, Cas12a *trans*-cleavage and SERS nanoprobes crosslinking can be integrated into a single and disposal vessel. It was proved that our proposed nanobioassay was able to detect SARS-CoV-2 as low as 200 copies/mL without any pre-amplification within 45

* Corresponding authors.
*E-mail addresses:* woshimalong1983@163.com, malong@tust.edu.cn (L. Ma), shenliang.0829@163.com (L. Shen), msl@tust.edu.cn (S. Man).

https://doi.org/10.1016/j.jhazmat.2023.131195
Received 14 January 2023; Received in revised form 8 March 2023; Accepted 10 March 2023
Available online 11 March 2023

min. In addition, the proposed nanobioassay was confirmed by clinical swab samples and challenged for SARS-CoV-2 detection in simulated complex environmental and food samples. This work enriches the arsenal of CRISPR-based diagnostics (CRISPR-Dx) and provides a novel and robust platform for SARS-CoV-2 decentralized detection, which can be put into practice in the near future.

## 1. Introduction

The coronavirus disease 2019 (COVID-19), caused by severe acute respiratory syndrome coronavirus 2 (SARS-CoV-2) infection, is an ongoing global pandemic and has spread more than 200 countries [1,2]. Therefore, rapid, sensitive, accurate and point-of-care (POC) detection of SARS-CoV-2 and emerging variants is vital for public safety and human health [3-6].

Clustered regularly interspaced short palindromic repeat (CRISPR)-associated (CRISPR/Cas) systems, deemed as the next generation diagnostic technology, have revolutionized the approaches that how pathogens can be detected [7,8]. CRISPR/Cas12a is a member of Class 2 type V CRISPR system. CRISPR/Cas12a specifically recognizes and cuts the target DNA under the guidance of a CRISPR RNA (crRNA), namely the *cis*-cleavage. Apart from this, CRISPR/Cas12a and crRNA binary complex is also known to possess a unique *trans*-cleavage effect (also named as collateral activity) upon recognizing and binding the target DNA sequence, leading to the indiscriminate shredding of any by-stander single-stranded DNA (ssDNA) [9]. By utilizing this *trans*-cleavage activity, a number of CRISPR/Cas-based diagnostics (CRISPR-Dx) strategies have been developed for a range of applications [10-19]. With the advantages of rapidity, simplicity, high sensitivity and specificity, CRISPR-Dx are also applied to SARS-CoV-2 detection in combination with different output readouts, such as fluorescent, colorimetric and electrochemical signals [20-25]. However, the most of these CRISPR-based detection methods depended on pre-amplification of target sequence. While the pre-amplification usually employs multiple enzymes, customized primers or expensive instruments; moreover, pre-amplification may cause amplification bias, which creates complexity for detection or results in non-linear distortions when profiling the original copy of nucleic acids. Highly sensitive and selective detection of infectious diseases without target pre-amplification owns advantages, which is worthy scientific studies [26]. To this end, some strategies have been designed, such as the application of combined crRNA, Fozouni et al. reported an amplification-free CRISPR/Cas13a method, which directly detected SARS-CoV-2 from nasal swab RNA that can be read by mobile phone microscope. The sensitivity of 100 copies/mL was reached within 30 min [27]. Choi et al. developed a CRISPR/Cas12a-assisted gold nanoparticle-assisted metal-enhanced fluorescence, which detected cfDNA sensitively (as low as 0.34 fM) and rapidly (30 min) without any pre-amplification [28], graphene field-effect-transistor [29,30], electrochemical microfluidic biosensor [31], electrochemiluminescence biosensor [32], microchamber-array [33], aptamer-assisted assay [34], autocatalysis-driven feedback amplification network [35], ultralocalized assay [36], and so on.

Surface-enhanced Raman scattering (SERS) is a signal enhancement technology, which can further improve the detection ability of Raman spectroscopy for low concentration biomolecules by manipulating the metal surface plasma effect [37]. Due to the enhancement of local electromagnetic field, noble metal nanomaterials such as gold nanoparticles (AuNPs) with rough surface can significantly enhance the Raman signals of probe molecules [38,39]. SERS measurement exhibits attractive superiority such as ultra-high sensitivity, unique fingerprint information and POC adaptability, and has been used as an advanced detection and characterization tool [40-42]. Taking the advantages of SERS, we previously reported a recombinase polymerase amplification (RPA) and CRISPR/Cas-integrated microfluidic paper-based analytical device (μPAD), coined RPA-Cas12a-μPAD for ultrasensitive and point-of-care detection of pathogenic bacteria [43].

However, most current strategies for CRISPR nucleic acid detection involve multiple steps, require lid opening to mix the reaction system, potentially causing cross-contamination. One vessel/tube detection module would, in this regard, improve the detection amenability by simplifying the detection process, avoiding the uncapping step, minimizing opportunistic aerosol contamination, and simplifying hands-on procedures. Some researchers have created a one-pot SHERLOCK by mixing RPA reagents and CRISPR reagents directly [44]. However, this may scarify the detection sensitivity. Innovation in experimental consumables is also an important approach. For example, Wang et al. integrated rapid PCR amplification and CRISPR/Cas12a *trans*-cleavage as one-pot reaction in capillary, so as to avoid the capping step of nucleic acid detection [45].

Herein, we described a novel one-vessel amplification-free CRISPR/Cas12a-powered SERS nanobioassay for SARS-CoV-2 detection, in which the steps of RNA reverse transcription, Cas12a *trans*-cleavage and SERS nanoprobes crosslinking can be integrated into a tube-in-tube reaction vessel. This nanobioassay was able to perform ultrasensitive, ultrafast, specific, quantitative, contamination-free and POC detection of SARS-CoV-2 at ambient temperature within around 45 min. It not only incorporated the sensitivity and specificity of CRISPR/Cas12a and SERS but also harnessed the simplicity, portability and quantitative capability of SERS detection. The entire detection process was streamlined and the customized vessel was easy-to-use in nucleic acid analysis.

## 2. Materials and methods

### 2.1. Materials

DNA oligonucleotides were synthesized by Sangon Biotech (Shanghai, China). Nucleic acid sequences were shown in Table S1. EnGen Lba Cas12a (Cpf1) from *Lachnospiraceae bacterium* ND2006 (#M0653T), HiScribeT7 Quick High Yield RNA Synthesis Kit (#E2050S) and Monarch® RNA Cleanup Kit (#T2040S) were purchased from New England Biolabs (USA). M-MLV Reverse Transcriptase (#M1701) was obtained from Promega (USA). Unless otherwise specified, the compounds used in this experiment were all obtained from Sigma-Aldrich (USA) or Aladdin Chem. Co., Ltd. (China). The bacterial and mammalian cell strains as well as pseudotyped viruses or plasmids used in this study were preserved and maintained in our laboratory.

### 2.2. Chemical synthesis and characterization of colloidal gold nanoparticles (AuNPs)

Different AuNPs were prepared according to method based on previous publications. Briefly, AuNPs with sizes 3 nm and 6 nm were prepared through the reduction of chloroauric acid ($HAuCl_4$) by sodium borohydride ($NaBH_4$) in the presence of a capping agent (sodium citrate). Typically, this involves the preparation of a 20 mL aqueous solution containing 0.25 mM $HAuCl_4$ and 0.25 mM sodium citrate. 0.6 mL and 0.4 mL of ice cold 0.1 M $NaBH_4$ was added into the above-mentioned aqueous solution, respectively for preparing 3 nm- and 6 nm-sized AuNPs. Upon the addition of $NaBH_4$, the solution immediately turned orange-red, indicating the formation of 3 nm and 6 nm AuNPs. After that, AuNPs with different sizes at 13, 20, 30, 50, 80 and 100 nm were prepared by the sodium citrate reduction method. Briefly, 100 μL of 1% $HAuCl_4$ was added to 30 mL of ultrapure water and brought to boiling. Next, 3, 2.5, 2, 1.5, and 1 mL of 1% sodium citrate was added to the solution to produce nanoparticles with the different sizes at 13, 20,

30, 50, 80 and 100 nm, respectively. The diameters of as-prepared AuNPs were confirmed by a Talos™ F200X G2 transmission electron microscope (TEM) and a Malvern ZS90 dynamic laser scattering (DLS), and further characterized by UV-Vis spectrophotometry.

### 2.3. Synthesis of SERS nanoprobes (AuNP@4-MBA@ssDNA)

20 nm AuNPs were prepared and the concentration (~1 nM) was determined by UV-Vis spectrophotometry [46]. The AuNP@ 4-MBA was obtained by adding 20 μL of 4-MBA (1 mM) solution into 1 mL AuNPs (~1 nM) under stirring at 37 °C for 2 h. Subsequently, AuNP@ 4-MBA@ssDNA were prepared by mixing 25 μL of thiolated DNA (100 μM) with 1 mL of AuNP@ 4-MBA and freezing at − 20°C for 2 h. The reaction was then maintained at room temperature and then was centrifuged at 12,000 rpm (10,000 g) for 20 min. The supernatant was discarded. The as-prepared AuNP@ 4-MBA@ssDNA was washed twice with buffer A (5 mM HEPES buffer, pH 7.6) to remove the excess ssDNA and re-suspended in 1 mL buffer B (10 mM HEPES buffer, 300 mM NaCl, pH 7.6) for use.

### 2.4. Production of SARS-CoV-2 pseudotyped viruses and determination of viral titer

SARS-CoV-2 pseudotyped viruses were produced and quantified according to the method of our previous study [22]. Simply, a lentiSARS-CoV-2-N plasmid was produced by cloning the SARS-CoV-2 N gene fragment into the PLVX-AcGFP-N1 vector. The SARS-CoV-2 pseudotyped viruses were generated by co-transfection of 293 T cells with 4 μg lentiSARS-CoV-2-N, 3 μg psPAX2 and 2 μg pMD2. G in 10 cm plates using TurboFect™ in vitro transfection reagent. 48 h later, the supernatant containing the pseudotyped viruses was collected and filtered (0.45 μm). The titer was determined by qPCR (Real-time quantitative PCR) method. To be detailed, 2 μL of pseudotyped viruses containing the SARS-CoV-2 N gene fragment were used template and mixed with qPCR mix containing 10 μL of 2 × T5 Fast qPCR Mix, 0.8 μL of forward primer/reverse primer (10 μM), 0.4 μL of DNA probe (10 μM), 0.4 μL of 50 × ROX Reference Dye I and 6.6 μL of nuclease-free water, which was then amplified using a StepOnePlus™ real-time PCR instrument. The limit of detection (LoD) was obtained based on a 3σ/k rule according to the International Union of Pure and Applied Chemistry (IUPAC) standard, where σ was the standard deviations of the blank samples, and k was the slop of the linear equation [47].

### 2.5. Design a tube-in-tube vessel for SARS-CoV-2 detection

The tube-in-tube vessel consisting of an inner and an outer tube was designed. The inner tube can be temporally immobilized inside the outer tube by a special locking structure. The lid of the inner tube was acted as the reaction container of reverse transcription, the inner tube was used as a storage vessel of CRISPR reagents and the reaction container of CRISPR/Cas12a cleavage, and the outer tube was used as the storage vessel of SERS nanoprobes and the final reaction container. A hole with one diameter of ~0.6 mm was located at the bottom of the inner tube, and a metal ball with a rod was used as a valve to control the opening and closing of the hole. The products of reverse transcription were mixed with the CRISPR reagents by turning the tube upside down. After the completion of CRISPR/Cas *trans*-cleavage of linker ssDNA, the valve of the inner tube could be opened by shaking, which allowed the solution in the inner tube to flow into the outer tube, where the final reaction generating SERS signals were carried out.

### 2.6. Test of some chemicals for CRISPR/Cas12a trans-cleavage activity enhancement

In order to achieve a chemically enhanced CRISPR/Cas-based detection, each chemical additive including betaine, DMSO (dimethyl sulfoxide), GABA (γ-aminobutyric acid), glycerol, PVA (polyvinyl alcohol), Tween-20 (Polysorbate 20), Triton X-100, L-proline was added to CRISPR/Cas12a reaction (200 nM Cas12a, 250 nM crRNA and 30 nM linker ssDNA in 10 mM HEPES buffer supplemented with 300 mM NaCl and 100 mM $MgCl_2$), respectively, which was incubated for 20 min to perform *trans*-cleavage of linker ssDNA. Other experimental procedures can be referred to Section 2.4.

### 2.7. SARS-CoV-2 detection with the proposed nanobioassay

Firstly, 200 μL of AuNP@ 4-MBA@ssDNA probes were added into the outer tube. Secondly, the inner tube was nested within the outer tube. 180 μL of Cas12a *trans*-cleavage reaction (200 nM Cas12a, 250 nM crRNA and 30 nM linker ssDNA in 10 mM HEPES buffer supplemented with 300 mM NaCl, 100 mM $MgCl_2$ and 0.5 M betaine) was added into the inner tube. Thirdly, 20 μL of reverse transcription reaction containing different concentrations of SARS-CoV-2 RNA (either from pseudotyped viruses or clinical samples) was dropped onto the lid of the inner tube for 20 min to complete reverse transcription (RT). Then, CRISPR/Cas12a *trans*-cleavage was triggered when mixing the reverse transcription products with CRISPR reagents by turning the tube upside down. After incubation at 37 °C for 20 min, the CRISPR/Cas12a *trans*-cleavage reaction was transferred into the outer tube by vigorously shaking, which was then incubated with SERS nanoprobes at 37 °C for 4 min. The final reaction solution in the outer tube was either centrifuged for 1 min or filtered with a 1.2 μm polyethersulfone (PES) membrane. Please note that the relative centrifugal force (RCF) was 850 *g*. The Raman signals of the supernatant or filtrate were obtained by a portable Raman spectrometer (Optosky ATR8300) with 150 mW power of excitation laser at 785 nm, 40 × objective and a 2 s accumulation time. Baseline correction and curve smoothing were switched on and performed automatically where necessary.

### 2.8. Clinical samples detection

This work has received approval for research ethics from the Ethical Committee of Xiangyang Central Hospital (#2021017) and the proof of approval is available upon request. A total of 100 clinical RNA samples extracted from de-identified nasopharyngeal swabs of confirmed COVID-19 cases and healthy individuals (50 samples for each) were provided by Xiangyang Central Hospital. The positive and negative samples were officially confirmed. The RNA was tested with the proposed nanobioassay, as described in Section 2.4. The cut-off value was the mean current change value of the background (experiment without using the target DNA, n = 3, B) plus three standard deviations (SD), B + 3 SD for determination of positivity and negativity [48].

### 2.9. Pseudotyped SARS-CoV-2 detection from environmental and food samples

300 μL of the solution containing different concentrations of SARS-CoV-2 pseudotyped viruses ($10^0$-$10^8$ copies/μL) was spiked into different samples, including frozen shrimp and cold-chain food packaging samples. For frozen shrimp samples, shrimp tissues (100 mg) spiked with pseudotyped SARS-CoV-2 were processed by a high-pressure homogenizer. The homogenate was centrifuged for 20 min at 4 °C. The RCF was 10,000 *g*. The supernatant was then filtered with a 0.22 μm filter before analysis. For cold-chain food packaging, round-shaped samples having a diameter of 3 cm each were scissored out, followed by the addition of droplets having pseudotyped SARS-CoV-2 of different concentrations ($10^0$-$10^8$ copies/μL) to simulate the contaminated samples. Then, each sample was rinsed with 200 μL of RNase-free distilled water in order to wash out the pseudotyped SARS-CoV-2 for collection. For environmental water samples, the water was collected from the Tianke river with in the campus of Tianjin University of Science and Technology, Tianjin, China, and then filtered with a 0.22 μm filter before

analysis. 300 μL of the environmental water samples were spiked with pseudotyped SARS-CoV-2 of different concentrations ($10^0$-$10^8$ copies/μL) were obtained. Total RNA of pseudotyped SARS-CoV-2 was extracted from each spiked sample using TIANamp Virus RNA Kit.

### 2.10. Repeatability and reproducibility evaluation

The same SARS-CoV-2 positive and negative samples were separately detected over 10 consecutive times with the proposed nanobioassay to evaluate the repeatability. Furthermore, the reproducibility was tested over different nanobioassays prepared at different times (n = 10 times, 1 time/each day). Relative standard deviation (RSD) was calculated accordingly.

### 2.11. Statistical analysis

The data obtained in the triplicated experiments were expressed as the mean ± standard deviation (SD) and analyzed by two-tailed Student's t-test where necessary. All statistical analyses were performed using the SPSS 17.0 software and P-value < 0.05 can be considered statistically significant.

## 3. Results and discussion

### 3.1. Design of the proposed OVER-SARS-CoV-2 nanobioassay

As illustrated in Scheme 1a, this proposed nanobioassay has two functional components, namely the activation of *trans*-cleavage of CRISPR/Cas12a and SERS-based detection. Simply, the viral RNA is extracted and reverse transcribed to obtain single-stranded (ss) complementary DNA (cDNA). Upon specific recognition of the target cDNA by Cas12a-crRNA binary complex, any ssDNA irrespective of sequence can be *trans*-cleaved. The designed ssDNA is tasked as a linker, hybridizing with the pre-made SERS nanoprobes respectively via complementary base pairing. The SERS nanoprobes are prepared by attaching the Raman reporter molecule 4-mercaptobenzoic acid (4-MBA) and thiolated ssDNA (DNA1 and DNA2) to AuNPs via Au-S bond. When the SARS-CoV-2 targets are present, the linker ssDNA would be shredded by the activated Cas12a in a non-specific manner, preventing the aggregation of SERS nanoprobes. The dispersed SERS nanoprobes would homogeneously distribute in the solution as stable colloidal particles even after mild centrifugation and thus can penetrate the filter membrane (pore size 1.2 μm). Therefore, the solution remains red-colored and generates strong SERS signals. On the contrary, the linker ssDNA remains intact in the absence of SARS-CoV-2 targets and the SERS nanoprobes would be crosslinked, inclining to aggregate and yielding precipitation after mild centrifugation or staying on the filter membrane after filtration. The solution, in this regard, becomes colorless and negligible SERS signals can be detected in the supernatant or filtrate. These SERS signals "turned on" by SARS-CoV-2 targets could be readily detected by a portable Raman spectrometer, easily adapting to on-site detection.

In order to streamline the detection processes, avoiding the lid-opening step to minimize the opportunistic aerosol pollution and

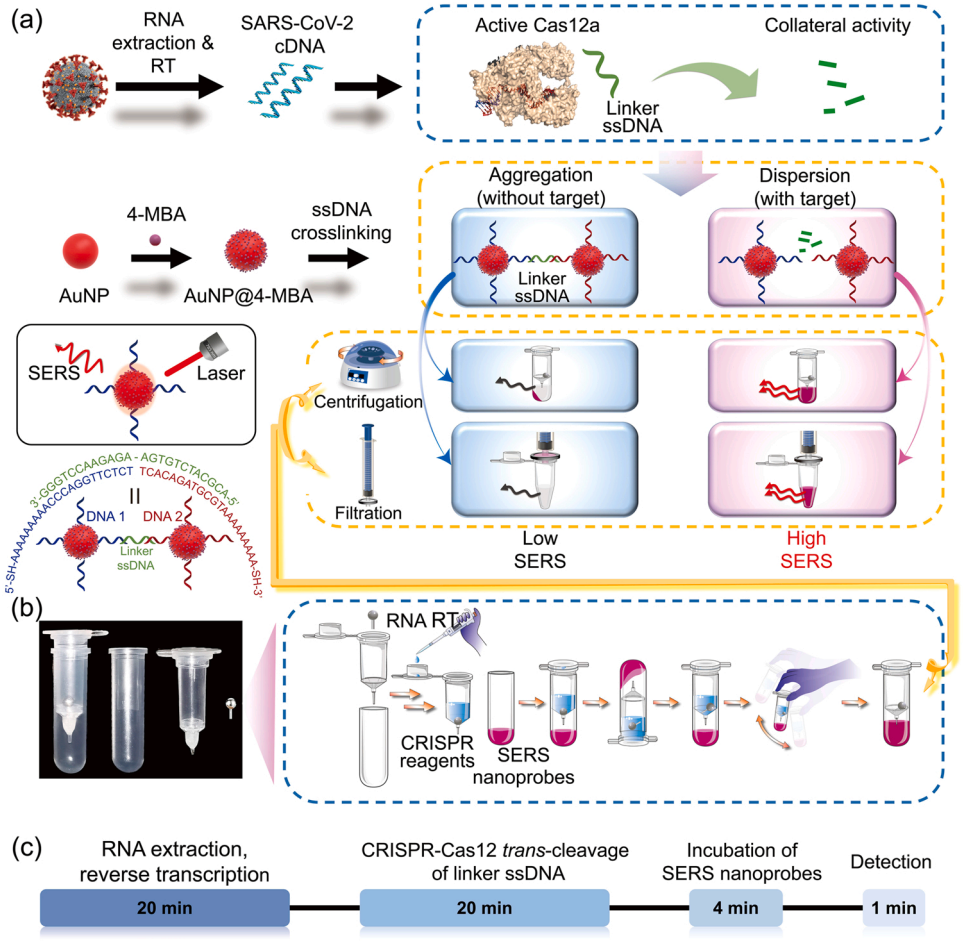


**Scheme 1.** The illustration of the proposed nanobioassay for SARS-CoV-2 detection in a single vessel. (a) The scheme of the proposed nanobioassay for amplification-free detection of SARS-CoV-2. (b) The picture of the designed tube-in-tube vessel (left) and the schematic showing the one-vessel detection of SARS-CoV-2 RNA (right). (c) The estimated time required for each step of the nanobioassay.

simplify the hands-on operation, a tube-in-tube vessel has been elaborately designed as shown in Scheme 1b. To be detailed, the SARS-CoV-2 RNA reverse transcription was carried out on the lid of the inner tube. After reverse transcription, the cDNA solution on the lid was mixed with the Cas12a cleavage reagents pre-stored in the inner tube by reversing the tube. After the completion of Cas12a cleavage, the reaction solution was permitted to enter the outer tube containing the pre-stalled SERS nanoprobes by vigorously shaking. Then, the solution in the outer tube was centrifuged or filtered (namely centrifugation method and filtration method, respectively) after a brief incubation and the Raman signals of the supernatant or filtrate were tested. The time needed for each step was represented in Scheme 1c.

### 3.2. Preparation, feasibility and optimization of the proposed nanobioassay

To prepare the proposed nanobioassay, SERS nanoprobes were firstly synthesized and characterized. AuNPs, employed as the SERS substrate, were modified with Raman reporting molecules 4-MBA and thiolated ssDNA as shown in Scheme 1. Fig. S1 showed chemical synthesis and characterization of different colloidal gold nanoparticles. The surface enhancement effect of AuNPs with different particle size was tested. We determined the optimal particle size of AuNPs was 20 nm (Fig. 1a). AuNP@ 4-MBA and AuNP@ 4-MBA@ssDNA were both characterized by energy dispersive X-ray (EDX)-TEM mapping, as shown in Fig. 1b. It was revealed S, O, and Au elements all existed, suggesting that the 4-MBA and ssDNA molecules were successfully conjugated within AuNPs. As shown in Fig. 1c, distinctive SERS peaks of 4-MBA at 1075, 1176, 1289, 1389, 1478 and 1587 $cm^{-1}$ were all significantly enhanced in AuNP@ 4-MBA, while naked AuNPs, 4-MBA as well the physical mixture of 4-MBA and naked AuNPs showed minimal Raman signals, reinforcing the necessity of bioconjugation of 4-MBA on the surface of AuNPs. The bands at 1075 and 1587 $cm^{-1}$ were respectively attributed to the in-plane ring breathing pattern coupled with $\nu$ (C-S) and the aromatic $\nu$ (C-C) vibrations pattern. The signals at 1075 $cm^{-1}$ wavenumber where the most intense peak appeared were adopted for plotting the histograms (Fig. 1d). Furthermore, the UV-Vis absorption spectra, dynamic laser scattering (DLS) and transmission electron microscope (TEM) were used to characterize the optical and morphological changes (Fig. 1e-h). The DLS data implied that the averaged diameter of naked AuNPs was 20.1 $\pm$ 0.4 nm. While AuNP@ 4-MBA and AuNP@ 4-MBA@ssDNA exhibited larger sizes of 61.2 $\pm$ 2.1 nm and 109.6 $\pm$ 3.6 nm, respectively. After adding the linker ssDNA, the SERS nanoprobes reached the largest sizes of 2670.4 $\pm$ 37.6 nm, indicating the successful hybridization between the linker ssDNA and the two kinds of SERS nanoprobes (Fig. 1g). The TEM observation was in agreement with the DLS characterization, which confirmed that the SERS nanoprobes aggregated after crosslinking (Fig. 1h). Moreover, We verified the fine storage stability of the as-prepared nanoprobes (stored at 4 $^{o}$C) for a 14-day time slot (Fig. S2).

Then, we incubated SERS nanoprobes with different concentrations of linker ssDNA to test the crosslinking effect. It was noted that the aggregation of the SERS nanoprobes occurred in the presence of linker ssDNA, which reached a plateau at the concentration of 30 nM. This indicated the complete hybridization between the linker ssDNA and SERS nanoprobes (Fig. 1i). The Raman signals also confirmed that the SERS nanoprobes were fully crosslinked in the presence of 30 nM linker ssDNA (Fig. 1j). Next, the feasibility of our nanobioassay was investigated. The plasmids carrying SARS-CoV-2 nucleocapsid (N) gene were firstly tested. As shown in Figs. 1k and 1 l, upon recognizing the SARS-CoV-2 N gene with the pre-designed crRNA (Fig. S3), the linker ssDNA was degraded non-specifically by the activated Cas12a as evidenced by the gel electrophoresis (Fig. S3), giving rise to high increase of Raman signals. To further raise the signal-to-noise ratio (SNR) of the proposed nanobioassay, several key experimental parameters were optimized. Fig. S4a showed the optimization of the Cas12a concentration. Fig. S4b showed the optimization of the incubation time of CRISPR/Cas12a and linker ssDNA. 20 min of *trans*-cleavage time and 200 nM concentration of Cas12a were finally chosen for subsequent use. It is reported that certain chemicals could enhanced the *trans*-ssDNA cleavage activity of Cas12a [49]. We therefore screened some non-ionic surfactants (e.g. Triton X-100, Tween and polyvinyl alcohol, PVA) and chemical additives (e.g. L-proline, glycerol) to obtain optimal condition for *trans*--cleavage of linker ssDNA. As shown in Fig. S5, it can be seen that the addition of betaine seemed to give a better response in SERS signals, which we decided to incorporate in the receipt of the buffer for subsequent use.

### 3.3. The performance of the proposed nanobioassay for SARS-CoV-2 detection

After the optimization of experimental conditions, the performance of the proposed nanobioassay was evaluated for SARS-CoV-2 detection, including sensitivity, quantitative capability, selectivity, repeatability and reproducibility. In the experiment, pseudotyped viruses containing the SARS-CoV-2 N gene were produced and tested. RT-qPCR was applied to determine the viral titer. Then, a series of diluted viral RNA from the pseudotyped viruses was reverse transcribed, followed by the detection using the proposed nanobioassay. Fig. 2a showed UV-Vis absorbance spectra change in the presence of pseudoviruses with various concentrations, which indicated UV-Vis method only can distinguish samples with concentration above $10^4$ copies/mL. This low sensitivity of UV-Vis method reinforced the need of SERS detection for probing low-viral load samples. Fig. 2b showed the color change in the presence of different concentrations of pseudotyped viruses before and after the centrifugation or filtration. In Fig. 2c, the SERS spectra showed an increase in Raman intensity with the increase of the concentration of SARS-CoV-2 pseudotyped viruses and the corresponding histogram (Raman intensity at 1075 $cm^{-1}$) was shown in Fig. 2d. The sensitivity of such detection reached 200 copies/mL. A linear association ($R^2$ = 0.983) between Raman intensity and SARS-CoV-2 the concentration of pseudotyped viruses was achieved over the ranges of $2 \times 10^2$-$10^8$ copies/mL (Fig. 2e).

In addition, to meet the needs of POC detection without requiring equipment, a filtration method other than centrifugation was performed to separate the SERS nanoprobes with different dispersion states (Fig. 2b right). We proposed that the dispersed SERS nanoprobes would penetrate the filter membrane (pore size 1.2 μm) and the aggregated SERS probes would be trapped on the filter membrane. The Raman signals of the liquid after filtration were tested. As shown in Fig. 2f, Raman intensity was correspondingly increased along with the increase of the concentration of SARS-CoV-2 RNA and a great linear association ($R^2$ = 0.944) between Raman intensity and SARS-CoV-2 RNA concentration was acquired (Fig. 2h). The detection limit was about $10^3$ copies/mL, which was slightly higher than the detection with a centrifugation method (Fig. 2g). The relative lower sensitivity and SERS intensity of the filtration method was probably caused by the excessive retention of SERS nanoprobes on filter membrane. Despite of this, the sensitivity of the proposed nanobioassay was comparable to those CRISPR-based detection methods with pre-amplification step [50] and was better than those previously reported amplification-free CRISPR-based methods [27,51] (summarized in Table S2 and S3). The superior sensitivity of the proposed nanobioassay can be attributed to the significant SERS enhancement provided by AuNP@ 4-MBA as well as the amplifying capability of CRISPR/Cas-based *trans*-cleavage upon target recognition. Different from the previous study that adopted SERS readouts in CRISPR/Cas-based nanobioassay [52], our proposed nanobioassay adopted a “turn-on” rather than a “turn-off” signal reporting approach, which would be more suitable for detecting nucleic acid samples with ultra-low copy numbers.

To check the selectivity, some other coronaviruses, such as SARS-CoV, Middle East respiratory syndrome coronavirus (MERS-CoV), and mouse hepatitis virus (MHV), influenza A virus (IAV), bacteria as well

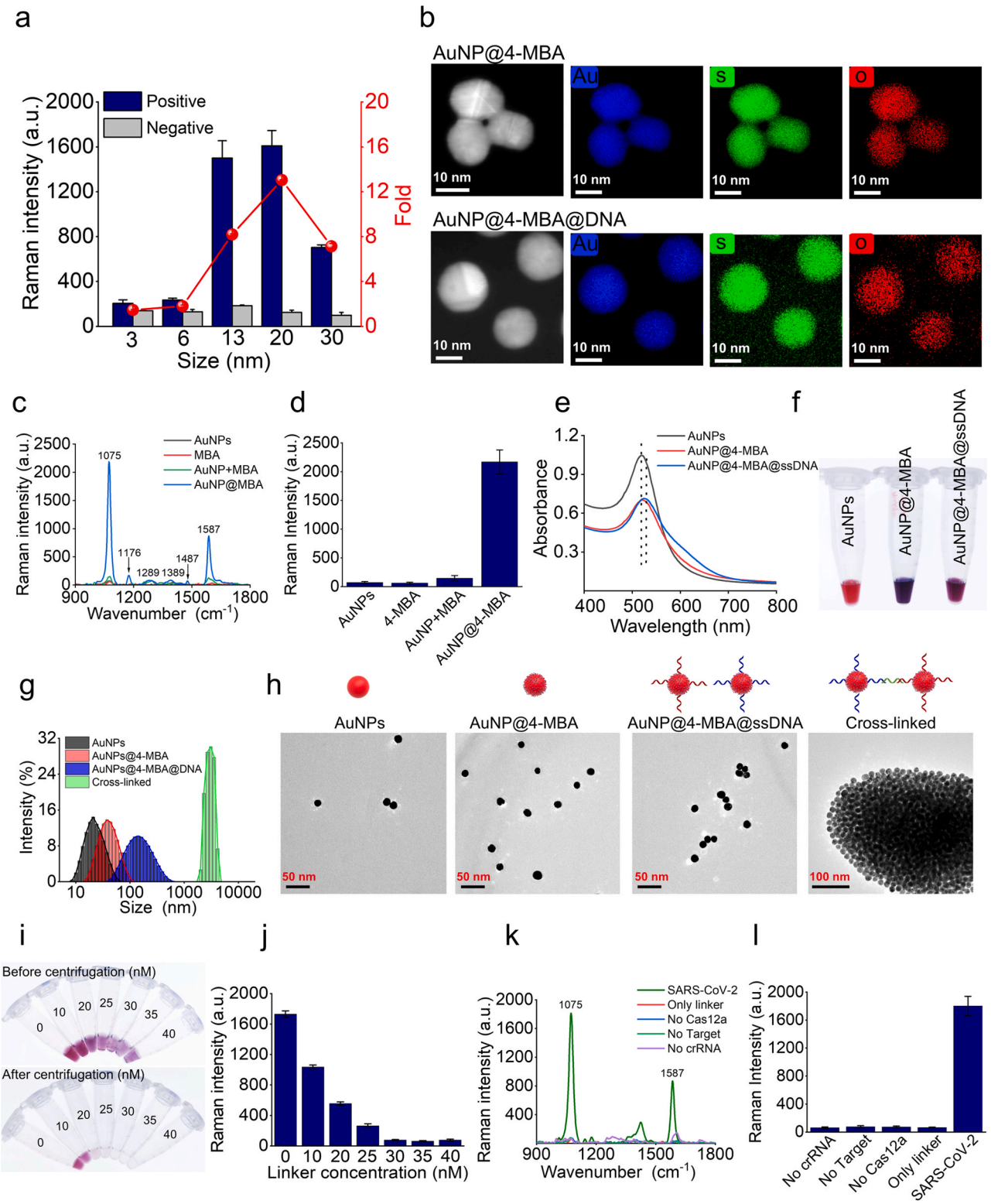


**Fig. 1.** Characterization of SERS nanoprobes and feasibility test of the proposed nanobioassay. **a:** Histogram of Raman signals responses to positive and negative samples at wavenumber of 1075 $cm^{-1}$ for AuNPs with different particle sizes. **b:** EDX-TEM mapping images of AuNP@ 4-MBA and AuNP@ 4-MBA@ssDNA nanoparticles. **c, d:** Raman spectra and histogram of Raman signals at wavenumber of 1075 $cm^{-1}$ of AuNPs, 4-MBA and AuNP@ 4-MBA nanoparticles. **e, f:** UV-Vis absorbance spectrum and picture of each sample. **g:** Dynamic laser scattering. **h:** Typical TEM images of AuNPs, AuNP@ 4-MBA, AuNP@ 4-MBA@ssDNA and the crosslinked AuNP@ 4-MBA@ssDNA. **i:** Different concentrations of linker ssDNA were incubated with AuNP@ 4-MBA@ssDNA nanoprobe pairs before and after centrifugation. **j:** The histogram of Raman intensity at wavenumber of 1075 $cm^{-1}$ of the supernatant after mild centrifugation. **k:** The feasibility assessment. Please note the plasmids carrying SARS-CoV-2 nucleocapsid (N) gene was used at 10 nM. **l:** The histogram of Raman intensity showed in Fig. 1k at wavenumber of 1075 $cm^{-1}$.

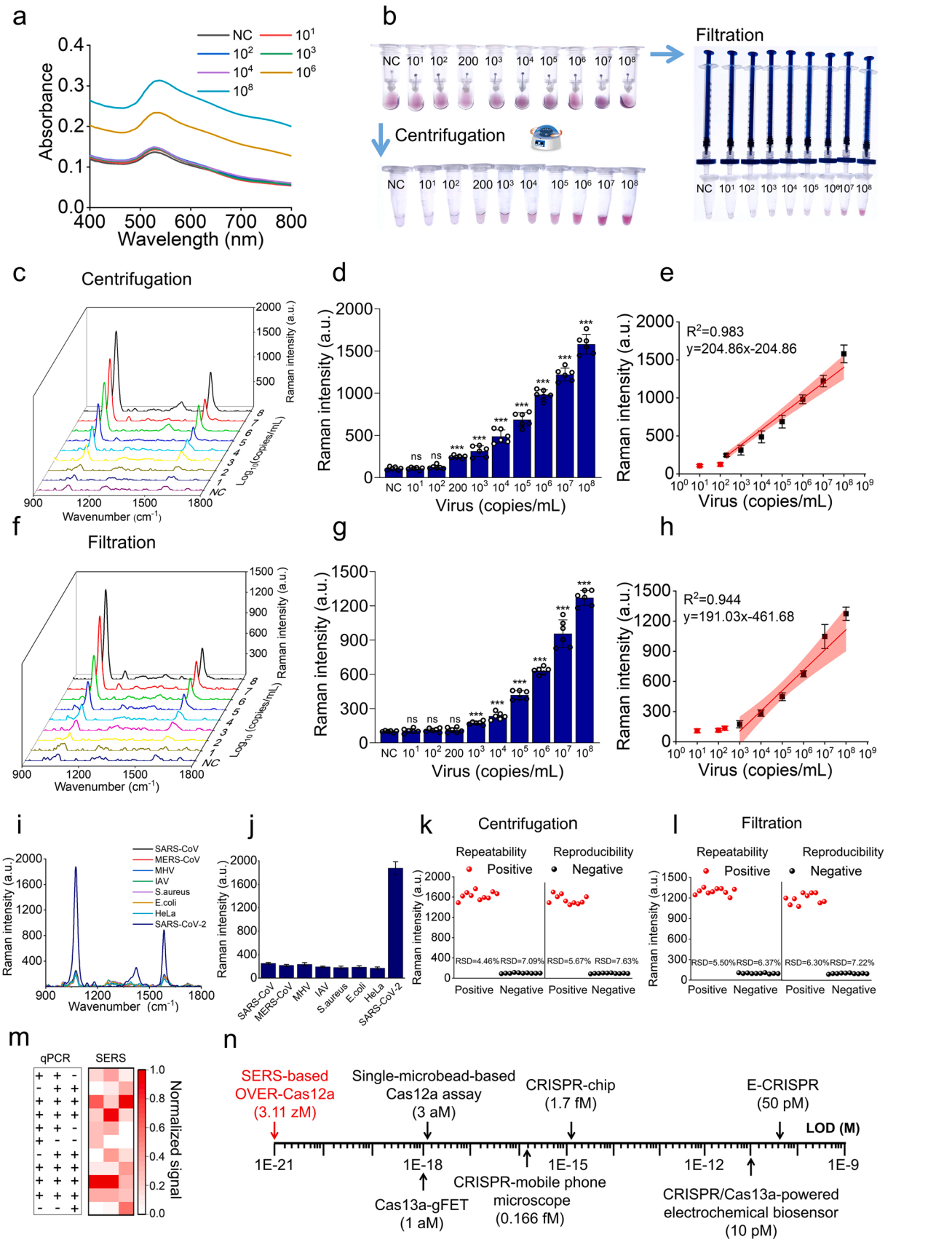


*(caption on next page)*

**Fig. 2.** The performance of SARS-CoV-2 pseudotyped viruses detection with the proposed nanobioassay. **a:** UV-Vis absorbance spectra to measure the AuNPs dispersion/aggregation for the proposed nanobioassay resulting from the pseudotyped viruses with various concentrations. **b:** The color changes of the solutions over the different concentrations of SARS-CoV-2 pseudotyped viruses before (top) and after centrifugation (bottom) or after filtration (right). **c, d:** Raman spectra and the corresponding histogram of Raman signals at wavenumber of 1075 $cm^{-1}$ for detection of SARS-CoV-2 pseudotyped viruses at different concentrations after centrifugation. **e:** The linear relationship between Raman intensity and the concentration of SARS-CoV-2 pseudotyped viruses obtained using the proposed bioassay with centrifugation. **f, g:** Raman spectra and the corresponding histogram of Raman signals at wavenumber of 1075 $cm^{-1}$ for quantitative detection of SARS-CoV-2 pseudotyped viruses at different concentrations after filtration. **h:** The linear relationship between Raman intensity and the concentration of SARS-CoV-2 pseudotyped viruses obtained using the proposed bioassay with filtration. **i, j:** The selectivity of the proposed bioassay (with centrifugation method) for SARS-CoV-2 over other respiratory viruses, bacteria and human cells. **k, l:** The repeatability and reproducibility of the proposed nanobioassay with centrifugation method and filtration method. **m:** Heat maps showing the comparison of SARS-CoV-2 pseudotyped viruses detection results of 33 samples with qPCR and the proposed bioassays. The "+ " and "− " respectively mean the qPCR positive and negative sample. n = 3 technical replicates; * $P < 0.05$, ** $P < 0.01$, *** $P < 0.001$; bars represent mean ± SD. Please note for qPCR testing, the cut-off was set as 40 Ct value, meaning that Ct value less than 40 and more than 40 can be considered positive and negative, respectively. ns = not significant. **n:** Comparison of the limit of detection (LoD) for various CRISPR-based bioassays without target preamplifications.

human cancer cells were examined. As shown in Fig. 2i-j, Raman intensity much increased exclusively only for SARS-CoV-2 samples, indicating that this nanobioassay was considerably selective toward SARS-CoV-2. Besides, the repeatability and reproducibility of the proposed OVER-SARS-CoV-2 with the centrifugation method and filtration method were both assessed and the RSD values were calculated as shown in Fig. 2k-l. All RSD values were less than 10% indicating that the proposed nanobioassay was reasonably repeatable and reproducible [53]. Furthermore, we compared the proposed nanobioassay with the classical qPCR method. Fig. 2m showed the proposed nanobioassay was 100% consistent with qPCR results. The LoD value our proposed nanobioassay (with centrifugation method) was calculated to be 1.9 copies/mL based on the 3σ/slope. The LoD value can be converted from "copies/mL concentration" to "molar concentration" as follows: (1.9 copies/mL)/(Avogadro constant) = 3.2 zM (please note: Avogadro constant was used as $6.022 \times 10^{23}$). Fig. 2n showed the comparison of the LoD values of for various amplification-free CRISPR-based bioassays [27,29,30,54,55,56]. To our knowledge, the LoD value onbtained with our proposed nanobioassay reached the lowest value ever, compared to other reported CRISPR/Cas-based amplification-free nucleic acid detection methods, which was of great significance.

### *3.4. The application of the proposed nanobioassay for the detection of SARS-CoV-2 clinical samples and beyond*

We further examined the proposed nanobioassay for clinical samples detection. A total of 100 clinical nasopharyngeal swab samples were tested, including 50 samples from COVID-19 positive cases and 50 samples from healthy persons, all of which were officially validated by the Hubei Center for Disease Control and Prevention (CDC), China. Viral RNA extracted from the swab samples was detected by the proposed nanobioassay (Fig. 3a). All positive samples tested using OVER-SARS-CoV-2 with centrifugation method and filtration method generated high Raman intensity; at the meantime, all 50 negative samples showed fairly low Raman intensity (namely 100% specificity) (Fig. 3b, c, d). The proposed nanobioassay can sensitively detect positive samples with cycle-threshold (Ct) values in the range from 35 to 36.6 that was usually considered as "grey zone", indicating that our proposed nanobioassay owned ultrahigh sensitivity for identifying the samples with ultralow viral loads. The clinical sensitivity of our proposed bioassay was 100% for both centrifugation and filtration methods (Fig. 3e). Moreover, there was an evident correlation between the Raman intensity and RT-qPCR Ct value (Fig. 3f-h).

Recent studies have shown that SARS-CoV-2 could persist in various environmental and food samples and retain infectivity for days to months, such as environmental water, cold-chain food and cold-chain food packaging [57,58]. The sensitive and specific detection of SARS-CoV-2 in such samples is of great importance for epidemic prevention and control. Here, we challenged the proposed nanobioassay for SARS-CoV-2 detection in three different actual samples, including environmental water, cold-chain food and food packaging. Simply, a series of concentrations of SARS-CoV-2 pseudotyped viruses were spiked into SARS-CoV-2-negative environmental water, frozen shrimp and food packaging samples to mimic viral contamination. For the detection of three different types of samples, an apparent increase in Raman intensity at $10^1$ copies/μL was achieved compared to that of the negative control group (Fig. S6). Besides, the Raman intensity increased linearly with the increased copies of SARS-CoV-2 pseudotyped viruses (Fig. S6). These indicated the ultrasensitive and robust detection properties of the proposed nanobioassay, which provided huge possibility for its practical and extensive applications.

CRISPR-Dx offers a promising alternative method for pathogenic nucleic acid detection, which owns extremely high sensitivity when coupling with pre-amplification step and are capable of detecting extremely low nucleic acids samples that are usually in the ambiguous "grey zone" of RT-qPCR ($35 < Ct < 40$) [59]. The nucleic acid amplification-free technique has its merits such as time-saving, less instrument dependency, exemption of polymerases and dNTPs, avoidance of unwanted off-template amplification products and secondary structures of primers, etc; moreover, it is also cost-effective and easy-to-operate [60]. The reported CRISPR-Dx without pre-amplification were summarized in Table S3. The conception of one-pot/tube/vessel detection is desirable in nucleic acid tests (NATs) owing to its simplicity, as well as fine capability of minimizing the risk of aerosol cross-contamination. Several CRISPR-based one-pot detection methods have been reported (summarized in Table S4). However, most of these methods are coupled with the pre-amplification step (e.g. RPA). The competition and interference between CRISPR detection and isothermal amplification might reduce the detection sensitivity [61]. The combination of both amplification-free and one-pot detection techniques would magnify their respective advantages but this usually suffers a serious shortcoming of poor sensitivity and specificity. In our work, to overcome this, we deliberately adopted the nucleic acids-targeting capability, sequence programmability, and target-induced biocatalytic signal amplifying capability of CRISPR/Cas12a to ingeniously convert SARS-CoV-2 RNA signals to SERS signals. The applications of "CRISPR/Cas" and "SERS" would serve as "belts and braces" to doubly ascertain the sensitivity and specificity. During the preparation of this manuscript, we noticed a recent published, in which they concluded that the amplification-free CRISPR/Cas12 detection would largely be governed by the fundamental nature of Cas12a *trans*-cleavage kinetics and the sensitivity of detection method [62]. It was hard for us to change the former; however, what we did in the current work focused on the latter by incorporating the high sensitivity of SERS within CRISPR-based assay, which just happened to agree well with what suggested in the work done by Santiago and co-workers. As far as we know, this work is the first report that integrates amplification-free detection in a one-pot fashion for fabricating CRISPR/Cas based SERS nanobioassays.

## 4. Conclusions

In this work, for the first time, we designed a one-vessel CRISPR/Cas12a-powered SERS nanobioassay for ultrasensitive detection of

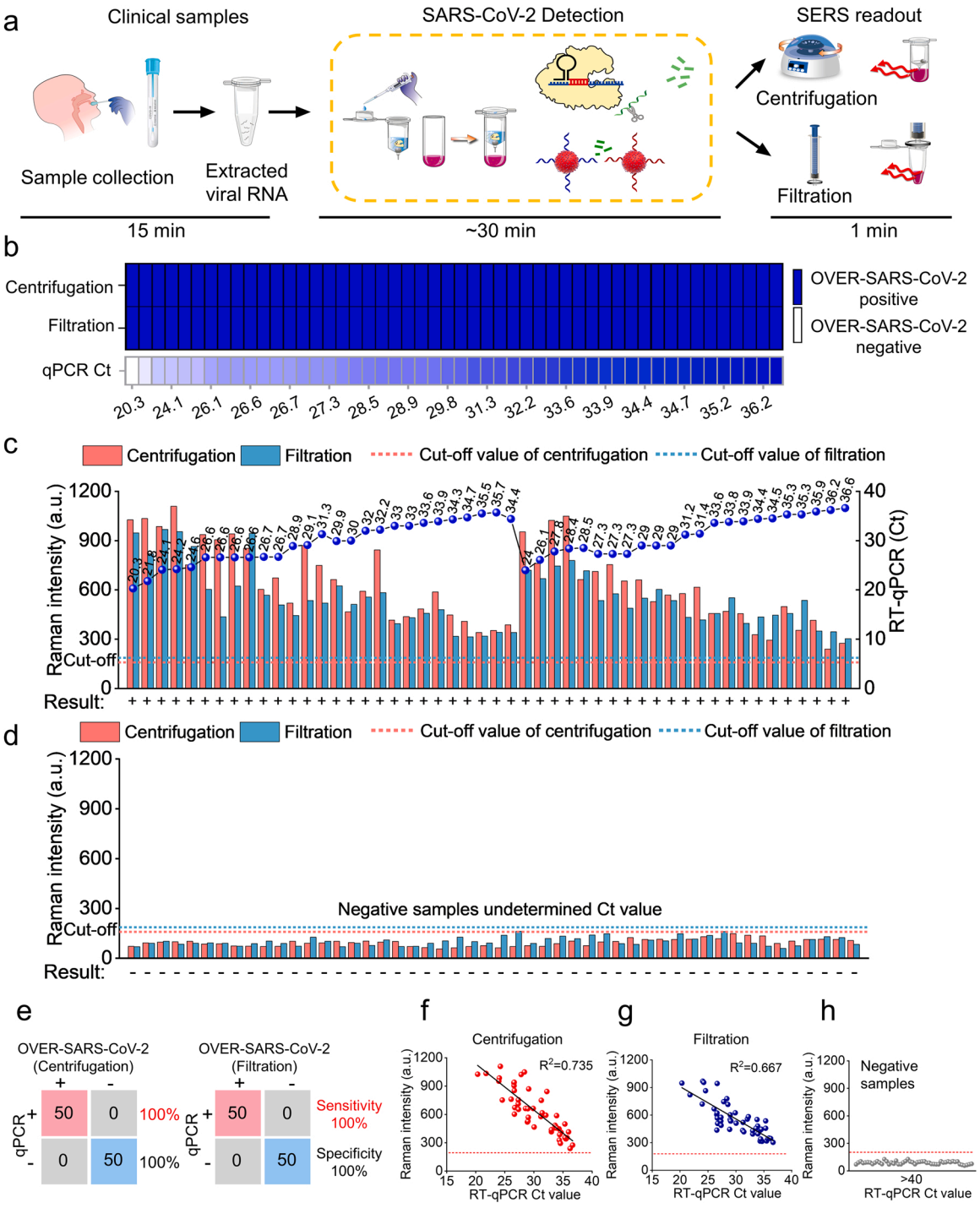


**Fig. 3.** The application of the proposed nanobioassay for detecting SARS-CoV-2 clinical samples. **a:** Schematic of the workflow for clinical samples detection using the proposed nanobioassay. **b:** Detection results of 50 COVID-19-positive clinical samples by the proposed nanobioassay and RT-qPCR (ordered by Ct value). **c, d:** Summary of the detection results of all clinical samples (50 COVID-19 positive samples and 50 negative samples) in comparison with RT-qPCR. **e:** Concordance tables between the proposed nanobioassay and RT-qPCR for 100 clinical samples. Sensitivity values (%) for the detection of the N genes are shown in red; specificity values (%) are shown in black. **f-h:** Correlation between RT-qPCR Ct value and Raman intensity for the detection of clinical samples. RT-qPCR positive samples (Ct range: 20–40) are plotted in color (red or blue), and RT-qPCR negative samples (Ct > 40) are plotted in grey.

SARS-CoV-2, with elimination of nucleic acid pre-amplification step. The devoid of pre-amplification did not sacrifice the detection sensitivity, as evidenced by the extremely low LoD value obtained in current study. On one hand, we explored the crRNA-mediated programmability, the target-induced non-specific DNA shredding ability of CRISPR/Cas12a, together with home-made nanoprobes for fabricating SERS-based biosensing strategy in order to obtain highly enhanced detection sensitivity. On the other hand, we devised a tube-in-tube low-cost reactor to accommodate the RNA reverse transcription, Cas12a *trans*-cleavage and nanoprobes dis-aggregation step-by-step in one vessel fashion for amplification-free and anti-interference detection. Moreover, its application can be verified by clinical samples as well as spiked environmental water and food samples. As such, the proposed nanobioassay balances the super-sensitivity, rapidity, specificity and on-site

detection potential, which potentially has the scalability for mass screening and can be easily implemented in resource-limited areas. This work opens a new CRISPR/Cas based detection paradigm and demonstrates how the application of nanomaterials can innovate biosensing thereof [63]. The logicalness and strategy can be extended for detecting various pathogenic microorganisms in the future [64,65].

## CRediT authorship contribution statement

**Long Ma**: Conceptualization, Investigation, Supervision, Methodology, Writing – original draft, Writing – review & editing, Funding acquisition. **Wenlu Zhang**: Experiment, Data analysis, Writing – original draft. **Lijuan Yin**: Investigation, Supervision, Writing – original draft. **Yaru Li**: Writing – review & editing. **Jianwen Zhuang**: Experiment. **Liang Shen**: Clinical samples. **Shuli Man**: Investigation, Supervision, Methodology.

## Declaration of Competing Interest

The authors declare that they have no known competing financial interests or personal relationships that could have appeared to influence the work reported in this paper.

## Data Availability

Data will be made available on request.

## Acknowledgments

This work was financially supported by National Natural Science Foundation of China (No. 32072309, 21672161, 81503086, 82002192), Tianjin Municipal Science and Technology Committee (19JCYBJC27800, 21JCQNJC01410, 22YFZCSN00070), State Key Laboratory of Food Nutrition and Safety, Tianjin University of Science & Technology (19PTSYJC00060), China Postdoctoral Science Foundation (2021M702460), Xiangyang Medical-health Areas Science and Technology Program (2020YL05).

*Declaration of competing interest*

The authors declare no competing financial interest.

## Appendix A. Supporting information

Supplementary data associated with this article can be found in the online version at doi:10.1016/j.jhazmat.2023.131195.

## References

[1] Hu, B., Guo, H., Zhou, P., Shi, Z.L., 2021. Characteristics of SARS-CoV-2 and COVID-19. Nat Rev Microbiol 19, 141–154.
[2] Li, Y., Qiao, J., Han, X., Zhao, Z., Kou, J., Zhang, W., Man, S., Ma, L., 2022. Needs, challenges and countermeasures of SARS-CoV-2 surveillance in cold-chain foods and packaging to prevent possible COVID-19 resurgence: A perspective from advanced detections. Viruses 15, 120.
[3] Ning, B., Yu, T., Zhang, S., Huang, Z., Tian, D., Lin, Z., Niu, A., Golden, N., Hensley, K., Threeton, B., Lyon, C.J., Yin, X.-M., Roy, C.J., Saba, N.S., Rappaport, J., Wei, Q., Hu, T.Y., 2021. A smartphone-read ultrasensitive and quantitative saliva test for COVID-19. Sci Adv 7, eabe3703.
[4] de Puig, H., Lee, R.A., Najjar, D., Tan, X., Soeknsen, L.R., Angenent-Mari, N.M., Donghia, N.M., Weckman, N.E., Ory, A., Ng, C.F., Nguyen, P.Q., Mao, A.S., Ferrante, T.C., Lansberry, G., Sallum, H., Niemi, J., Collins, J.J., 2021. Minimally instrumented SHERLOCK (miSHERLOCK) for CRISPR-based point-of-care diagnosis of SARS-CoV-2 and emerging variants. Sci Adv 7, eabh2944.
[5] Wang, Y., Zhang, Y., Chen, J., Wang, M., Zhang, T., Luo, W., Li, Y., Wu, Y., Zeng, B., Zhang, K., Deng, R., Li, W., 2021. Detection of SARS-CoV-2 and its mutated variants via CRISPR-Cas13-based transcription amplification. Anal Chem 93, 3393–3402.
[6] Yang, T., Li, D., Yan, Y., Ettoumi, F.E., Wu, R.A., Luo, Z., Yu, H., Lin, X., 2023. Ultrafast and absolute quantification of SARS-CoV-2 on food using hydrogel RT-LAMP without pre-lysis. J Hazard Mater 442, 130050.
[7] Li, Y., Liao, D., Kou, J., Tong, Y., Daniels, L.C., Man, S., Ma, L., 2022. Comparison of CRISPR/Cas and argonaute for nucleic acid tests. Trends Biotechnol.
[8] Yin, L., Man, S., Ye, S., Liu, G., Ma, L., 2021. CRISPR-Cas based virus detection: Recent advances and perspectives. Biosens Bioelectron 193, 113541.
[9] Chen, J.S., Ma, E., Harrington, L.B., Da Costa, M., Tian, X., Palefsky, J.M., Doudna, J.A., 2018. CRISPR-Cas12a target binding unleashes indiscriminate single-stranded DNase activity. Science 360, 436–439.
[10] Du, Y.C., Wang, S.Y., Wang, Y.X., Ma, J.Y., Wang, D.X., Tang, A.N., Kong, D.M., 2021. Terminal deoxynucleotidyl transferase combined CRISPR-Cas12a amplification strategy for ultrasensitive detection of uracil-DNA glycosylase with zero background. Biosens Bioelectron 171, 112734.
[11] Kaminski, M.M., Abudayyeh, O.O., Gootenberg, J.S., Zhang, F., Collins, J.J., 2021. CRISPR-based diagnostics. Nat Biomed Eng 5, 643–656.
[12] Li, Y., Li, S., Wang, J., Liu, G., 2019. CRISPR/Cas Systems towards next-generation biosensing. Trends Biotechnol 37, 730–743.
[13] Ma, L., Peng, L., Yin, L., Liu, G., Man, S., 2021. CRISPR-Cas12a-powered dual-mode biosensor for ultrasensitive and cross-validating detection of pathogenic bacteria. ACS Sens 6, 2920–2927.
[14] Ma, L., Wang, J., Li, Y., Liao, D., Zhang, W., Han, X., Man, S., 2023. A ratiometric fluorescent biosensing platform for ultrasensitive detection of *Salmonella typhimurium* via CRISPR/Cas12a and silver nanoclusters. J Hazard Mater 443, 130234.
[15] Peng, L., Zhou, J., Yin, L., Man, S., Ma, L., 2020. Integration of logic gates to CRISPR/Cas12a system for rapid and sensitive detection of pathogenic bacterial genes. Anal Chim Acta 1125, 162–168.
[16] Peng, L., Zhou, J., Liu, G., Yin, L., Ren, S., Man, S., Ma, L., 2020. CRISPR-Cas12a based aptasensor for sensitive and selective ATP detection. Sens Actuators B Chem 320, 128164.
[17] Phan, Q.A., Truong, L.B., Medina-Cruz, D., Dincer, C., Mostafavi, E., 2022. CRISPR/Cas-powered nanobiosensors for diagnostics. Biosens Bioelectron 197, 113732.
[18] Wang, Y., Peng, Y., Li, S., Han, D., Ren, S., Qin, K., Zhou, H., Han, T., Gao, Z., 2023. The development of a fluorescence/colorimetric biosensor based on the cleavage activity of CRISPR-Cas12a for the detection of non-nucleic acid targets. J Hazard Mater 449, 131044.
[19] Yin, L., Duan, N., Chen, S., Yao, Y., Liu, J., Ma, L., 2021. Ultrasensitive pathogenic bacteria detection by a smartphone-read G-quadruplex-based CRISPR-Cas12a bioassay. Sens Actuators B Chem 347, 130586.
[20] Joung, J., Ladha, A., Saito, M., Kim, N.-G., Woolley, A.E., Segel, M., Barretto, R.P. J., Ranu, A., Macrae, R.K., Faure, G., Ioannidi, E.I., Krajeski, R.N., Bruneau, R., Huang, M.-L.W., Yu, X.G., Li, J.Z., Walker, B.D., Hung, D.T., Greninger, A.L., Jerome, K.R., Gootenberg, J.S., Abudayyeh, O.O., Zhang, F., 2020. Detection of SARS-CoV-2 with SHERLOCK one-pot testing. N Engl J Med 383, 1492–1494.
[21] Liu, J., Wang, H., Zhang, L., Lu, Y., Wang, X., Shen, M., Li, N., Feng, L., Jing, J., Cao, B., Zou, X., Cheng, J., Xu, Y., 2022. Sensitive and rapid diagnosis of respiratory virus coinfection using a microfluidic chip-powered CRISPR/Cas12a system. Small 18, e2200854.
[22] Ma, L., Yin, L., Li, X., Chen, S., Peng, L., Liu, G., Ye, S., Zhang, W., Man, S., 2022. A smartphone-based visual biosensor for CRISPR-Cas powered SARS-CoV-2 diagnostics. Biosens Bioelectron 195, 113646.
[23] Su, J., Ke, Y., Maboyi, N., Zhi, X., Yan, S., Li, F., Zhao, B., Jia, X., Song, S., Ding, X., 2021. CRISPR/Cas12a powered DNA framework-supported electrochemical biosensing platform for ultrasensitive nucleic acid analysis. Small Methods 5, e2100935.
[24] Yang, Y., Liu, J., Zhou, X., 2021. A CRISPR-based and post-amplification coupled SARS-CoV-2 detection with a portable evanescent wave biosensor. Biosens Bioelectron 190, 113418.
[25] Zhang, K., Fan, Z., Ding, Y., Xie, M., 2022. A pH-engineering regenerative DNA tetrahedron ECL biosensor for the assay of SARS-CoV-2 RdRp gene based on CRISPR/Cas12a trans-activity. Chem Eng J 429, 132472.
[26] Morales-Narvaez, E., Dincer, C., 2020. The impact of biosensing in a pandemic outbreak: COVID-19. Biosens Bioelectron 163, 112274.
[27] Fozouni, P., Son, S., Diaz de Leon Derby, M., Knott, G.J., Gray, C.N., D'Ambrosio, M.V., Zhao, C., Switz, N.A., Kumar, G.R., Stephens, S.I., Boehm, D., Tsou, C.L., Shu, J., Bhuiya, A., Armstrong, M., Harris, A.R., Chen, P.Y., Osterloh, J. M., Meyer-Franke, A., Joehnk, B., Walcott, K., Sil, A., Langelier, C., Pollard, K.S., Crawford, E.D., Puschnik, A.S., Phelps, M., Kistler, A., DeRisi, J.L., Doudna, J.A., Fletcher, D.A., Ott, M., 2021. Amplification-free detection of SARS-CoV-2 with CRISPR-Cas13a and mobile phone microscopy. Cell 184, 323–333 e329.
[28] Choi, J.H., Lim, J., Shin, M., Paek, S.H., Choi, J.W., 2021. CRISPR-Cas12a-based nucleic acid amplification-free DNA biosensor via Au nanoparticle-assisted metal-enhanced fluorescence and colorimetric analysis. Nano Lett 21, 693–699.
[29] Hajian, R., Balderston, S., Tran, T., deBoer, T., Etienne, J., Sandhu, M., Wauford, N. A., Chung, J.Y., Nokes, J., Athaiya, M., Paredes, J., Peytavi, R., Goldsmith, B., Murthy, N., Conboy, I.M., Aran, K., 2019. Detection of unamplified target genes via CRISPR-Cas9 immobilized on a graphene field-effect transistor. Nat Biomed Eng 3, 427–437.
[30] Li, H., Yang, J., Wu, G., Weng, Z., Song, Y., Zhang, Y., Vanegas, J.A., Avery, L., Gao, Z., Sun, H., Chen, Y., Dieckhaus, K.D., Gao, X., Zhang, Y., 2022. Amplification-free detection of SARS-CoV-2 and respiratory syncytial virus using CRISPR Cas13a and graphene field-effect transistors. Angew Chem Int Ed Engl 61, e202203826.
[31] Bruch, R., Baaske, J., Chatelle, C., Meirich, M., Madlener, S., Weber, W., Dincer, C., Urban, G.A., 2019. CRISPR/Cas13a-powered electrochemical microfluidic biosensor for nucleic acid amplification-free miRNA diagnostics. Adv Mater 31, e1905311.

[32] Liu, P.F., Zhao, K.R., Liu, Z.J., Wang, L., Ye, S.Y., Liang, G.X., 2021. Cas12a-based electrochemiluminescence biosensor for target amplification-free DNA detection. Biosens Bioelectron 176, 112954.
[33] Shinoda, H., Taguchi, Y., Nakagawa, R., Makino, A., Okazaki, S., Nakano, M., Muramoto, Y., Takahashi, C., Takahashi, I., Ando, J., Noda, T., Nureki, O., Nishimasu, H., Watanabe, R., 2021. Amplification-free RNA detection with CRISPR-Cas13. Commun Biol 4, 476.
[34] Wei, Y., Tao, Z., Wan, L., Zong, C., Wu, J., Tan, X., Wang, B., Guo, Z., Zhang, L., Yuan, H., Wang, P., Yang, Z., Wan, Y., 2022. Aptamer-based Cas14a1 biosensor for amplification-free live pathogenic detection. Biosens Bioelectron 211, 114282.
[35] Shi, K., Xie, S., Tian, R., Wang, S., Lu, Q., Gao, D., Lei, C., Zhu, H., Nie, Z., 2021. A CRISPR-Cas autocatalysis-driven feedback amplification network for supersensitive DNA diagnostics. Sci Adv 7, eabc7802.
[36] Tian, T., Shu, B., Jiang, Y., Ye, M., Liu, L., Guo, Z., Han, Z., Wang, Z., Zhou, X., 2021. An ultralocalized Cas13a assay enables universal and nucleic acid amplification-free single-molecule RNA diagnostics. ACS Nano 15, 1167–1178.
[37] Zong, C., Xu, M., Xu, L.-J., Wei, T., Ma, X., Zheng, X.-S., Hu, R., Ren, B., 2018. Surface-enhanced Raman spectroscopy for bioanalysis: reliability and challenges. Chem Rev 118, 4946–4980.
[38] Guselnikova, O., Lim, H., Kim, H.J., Kim, S.H., Gorbunova, A., Eguchi, M., Postnikov, P., Nakanishi, T., Asahi, T., Na, J., Yamauchi, Y., 2022. New trends in nanoarchitectured SERS substrates: nanospaces, 2D materials, and organic heterostructures. Small 18, e2107182.
[39] Xu, T., Luo, Y., Liu, C., Zhang, X., Wang, S., 2020. Integrated ultrasonic aggregation-induced enrichment with Raman enhancement for ultrasensitive and rapid biosensing. Anal Chem 92, 7816–7821.
[40] Guo, X., Li, J., Arabi, M., Wang, X., Wang, Y., Chen, L., 2020. Molecular-imprinting-based surface-enhanced Raman scattering sensors. ACS Sens 5, 601–619.
[41] Liu, J., Chen, J., Wu, D., Huang, M., Chen, J., Pan, R., Wu, Y., Li, G., 2021. CRISPR-/Cas12a-mediated liposome-amplified strategy for the surface-enhanced raman scattering and naked-eye detection of nucleic acid and application to food authenticity screening. Anal Chem 93, 10167–10174.
[42] Yang, Y., Peng, Y., Lin, C., Long, L., Hu, J., He, J., Zeng, H., Huang, Z., Li, Z.Y., Tanemura, M., Shi, J., Lombardi, J.R., Luo, X., 2021. Human ACE2-functionalized gold "virus-trap" nanostructures for accurate capture of SARS-CoV-2 and single-virus SERS detection. Nanomicro Lett 13, 109.
[43] Zhuang, J., Zhao, Z., Lian, K., Yin, L., Wang, J., Man, S., Liu, G., Ma, L., 2022. SERS-based CRISPR/Cas assay on microfluidic paper analytical devices for supersensitive detection of pathogenic bacteria in foods. Biosens Bioelectron 207, 114167.
[44] Kellner, M.J., Koob, J.G., Gootenberg, J.S., Abudayyeh, O.O., Zhang, F., 2019. SHERLOCK: nucleic acid detection with CRISPR nucleases. Nat Protoc 14, 2986–3012.
[45] Wang, R., Chen, R., Qian, C., Pang, Y., Wu, J., Li, F., 2021. Ultrafast visual nucleic acid detection with CRISPR/Cas12a and rapid PCR in single capillary. Sens Actuators B Chem 326, 128618.
[46] Haiss, W., Thanh, N.T.K., Aveyard, J., Fernig, D.G., 2007. Determination of size and concentration of gold nanoparticles from UV−Vis spectra. Anal Chem 79, 4215–4221.
[47] Araujo, P., 2009. Key aspects of analytical method validation and linearity evaluation. J Chromatogr B 877, 2224–2234.
[48] Zhang, Q., Li, J., Li, Y., Tan, G., Sun, M., Shan, Y., Zhang, Y., Wang, X., Song, K., Shi, R., Huang, L., Liu, F., Yi, Y., Wu, X., 2022. SARS-CoV-2 detection using quantum dot fluorescence immunochromatography combined with isothermal amplification and CRISPR/Cas13a. Biosens Bioelectron 202, 113978.
[49] Deng, F., Li, Y., Li, B., Goldys, E.M., 2022. Increasing trans-cleavage catalytic efficiency of Cas12a and Cas13a with chemical enhancers: application to amplified nucleic acid detection. Sens Actuators B Chem 373, 132767.
[50] Broughton, J.P., Deng, X., Yu, G., Fasching, C.L., Servellita, V., Singh, J., Miao, X., Streithorst, J.A., Granados, A., Sotomayor-Gonzalez, A., Zorn, K., Gopez, A., Hsu, E., Gu, W., Miller, S., Pan, C.Y., Guevara, H., Wadford, D.A., Chen, J.S., Chiu, C.Y., 2020. CRISPR-Cas12-based detection of SARS-CoV-2. Nat Biotechnol 38, 870–874.
[51] Silva, F.S.R., Erdogmus, E., Shokr, A., Kandula, H., Thirumalaraju, P., Kanakasabapathy, M.K., Hardie, J.M., Pacheco, L.G.C., Li, J.Z., Kuritzkes, D.R., Shafiee, H., 2021. SARS-CoV-2 RNA detection by a cellphone-based amplification-free system with CRISPR/CAS-Dependent Enzymatic (CASCADE) assay. Adv Mater Technol 6, 2100602.
[52] Liang, J., Teng, P., Xiao, W., He, G., Song, Q., Zhang, Y., Peng, B., Li, G., Hu, L., Cao, D., Tang, Y., 2021. Application of the amplification-free SERS-based CRISPR/Cas12a platform in the identification of SARS-CoV-2 from clinical samples. J Nanobiotechnol 19, 273.
[53] Ghorbanizamani, F., Moulahoum, H., Zihnioglu, F., Evran, S., Cicek, C., Sertoz, R., Arda, B., Goksel, T., Turhan, K., Timur, S., 2021. Quantitative paper-based dot blot assay for spike protein detection using fuchsine dye-loaded polymersomes. Biosens Bioelectron 192, 113484.
[54] Liu, L., Xu, Z., Awayda, K., Dollery, S.J., Bao, M., Fan, J., Cormier, D., O'Connell, M., Tobin, G.J., Du, K., 2022. Gold nanoparticle-labeled CRISPR-Cas13a assay for the sensitive solid-state nanopore molecular counting. Adv Mater Technol 7, 2101550.
[55] Mohammad, N., Katkam, S.S., Wei, Q., 2022. A sensitive and nonoptical CRISPR detection mechanism by sizing double-stranded lambda DNA reporter. Angew Chem Int Ed Engl 61, e202213920.
[56] Yang, X., Li, J., Zhang, S., Li, C., Ma, J., 2022. Amplification-free, single-microbead-based Cas12a assay for one-step DNA detection at the single-molecule level. Anal Chem 94, 13076–13083.
[57] Mohan, S.V., Hemalatha, M., Kopperi, H., Ranjith, I., Kumar, A.K., 2021. SARS-CoV-2 in environmental perspective: Occurrence, persistence, surveillance, inactivation and challenges. Chem Eng J 405, 126893.
[58] Pang, X., Ren, L., Wu, S., Ma, W., Yang, J., Di, L., Li, J., Xiao, Y., Kang, L., Du, S., Du, J., Wang, J., Li, G., Zhai, S., Chen, L., Zhou, W., Lai, S., Gao, L., Pan, Y., Wang, Q., Li, M., Wang, J., Huang, Y., Wang, J., Group, C.-F.R., Group, C.-L.T., 2020. Cold-chain food contamination as the possible origin of COVID-19 resurgence in Beijing. Natl Sci Rev 7, 1861–1864.
[59] Chen, Y., Wu, S., Wu, H., Cheng, P., Wang, X., Qian, S., Zhang, M., Xu, J., Ji, F., Wu, J., 2021. CRISPR/Cas12a-based versatile method for checking quantitative polymerase chain reaction samples with cycles of threshold values in the gray zone. ACS Sens 6, 1963–1970.
[60] Qian, S., Chen, Y., Xu, X., Peng, C., Wang, X., Wu, H., Liu, Y., Zhong, X., Xu, J., Wu, J., 2022. Advances in amplification-free detection of nucleic acid: CRISPR/Cas system as a powerful tool. Anal Biochem 643, 114593.
[61] Lu, S., Tong, X., Han, Y., Zhang, K., Zhang, Y., Chen, Q., Duan, J., Lei, X., Huang, M., Qiu, Y., Zhang, D.Y., Zhou, X., Zhang, Y., Yin, H., 2022. Fast and sensitive detection of SARS-CoV-2 RNA using suboptimal protospacer adjacent motifs for Cas12a. Nat Biomed Eng 6, 286–297.
[62] Huyke, D.A., Ramachandran, A., Bashkirov, V.I., Kotseroglou, E.K., Kotseroglou, T., Santiago, J.G., 2022. Enzyme kinetics and detector sensitivity determine limits of detection of amplification-free CRISPR-Cas12 and CRISPR-Cas13 diagnostics. Anal Chem 94, 9826–9834.
[63] Zhang, X., Shi, Y., Chen, G., Wu, D., Wu, Y., Li, G., 2022. CRISPR/Cas systems-inspired Nano/Biosensors for detecting infectious viruses and pathogenic bacteria. Small Methods, e2200794.
[64] Li, Y., Zhang, W., Han, X., Wu, Q., Xie, Y., Fan, J., Ma, L., 2023. Detection methods for foodborne viruses: Current state-of-art and future perspectives. J. Agric. Food Chem. 71, 3551–3563.
[65] Tan, J., Liu, L., Li, F., Chen, Z., Chen, G.Y., Fang, F., Guo, J., He, M., Zhou, X., 2022. Screening of endocrine disrupting potential of surface waters via an affinity-based biosensor in a rural community in the Yellow River Basin, China. Environ Sci Technol 56, 14350–14360.